Journal of Alloys and Compounds 512 (2012) 156–159

Contents lists available at SciVerse ScienceDirect

Journal of Alloys and Compounds

journal homepage: www.elsevier.com/locate/jallcom

A novel approach to co-sintering of doped lanthanum chromite interconnect on Ni–YSZ anode substrate for SOFC applications

A. Heidarpour[a,*], G.M. Choi[b], M.H. Abbasi[a], A. Saidi[a]

[a] Department of Materials Engineering, Isfahan University of Technology (IUT), Isfahan 84156-83111, Iran
[b] Fuel Cell Research Center and Department of Materials Science and Engineering, Pohang University of Science and Technology, Pohang 790-784, Republic of Korea

ARTICLE INFO

Article history:
Received 12 July 2011
Received in revised form
18 September 2011
Accepted 19 September 2011
Available online 22 September 2011

Keywords:
Interconnect material
Co-sintering
Lanthanum chromite
Electrical properties

ABSTRACT

A cost-effective method was developed to fabricate dense doped $LaCrO_3$ bases interconnect membrane on anode substrate for solid oxide fuel cell (SOFC) applications. As conventional lanthanum chromite interconnect is difficult to be co-sintered with green anode, a simple and cost effective screen printing/co-sintering process was employed, and dense $La_{1-x-y}Sr_xCa_yCrO_{3-\delta}$ interconnect membrane was successfully prepared on the anode support of NiO–YSZ. In this method a base layer of doped lanthanum chromite ($La_{1-x}Sr_xCrO_{3-\delta}$) was applied on NiO–YSZ substrate and a top layer of $CaCrO_4$ was then coated and co-sintered to melt the top layer. By means of this method, not only $CaCrO_4$ melts and fills the open pores in the base layer, but it also dissolves in base layer forming $La_{1-x-y}Sr_xCa_yCrO_{3-\delta}$ as a single layer. The sintering characteristics, microstructure and electrical conductivity of interconnect were investigated. In addition, the effects of composition on sintering and electrical properties were studied.

1. Introduction

Solid oxide fuel cells (SOFCs) have been developed as an advanced technology for clean, high efficient and reliable energy conversion. In this research field, exciting progress has been achieved so far on individual cells, such as high performance and novel designs [1–3]. The SOFCs can be constructed with either a tubular or a planar design. The tubular design has been used for small to large-scale power generation systems and has many advantages such as the ease of sealing and ability to endure the thermal stress caused by rapid heating [4–6]. However, for tubular SOFC stacks, only ceramic interconnect can be used [7]. This part of SOFC still remains to be a main challenge holding back single fuel cells from being compiled into stacks [8]. Interconnector provides the conductive path for electrical current to pass from the anode of one cell to the cathode of the next one, as well as separating the fuel gas from the oxidant. So, it should be completely dense, sufficiently conductive, and quite stable in both oxidizing and reducing atmospheres. Due to these tough requirements, only few materials can be used for SOFC interconnector. Lanthanum chromite ($LaCrO_3$) based perovskite materials are the most promising which have high thermal and chemical stability in dual oxidation–reduction atmosphere as well as good electrical conductivity; thus, they have been extensively investigated [9–12]. However, their poor sintering ability makes them unable to be co-sintered with green tubular anode, resulting in a high cost for manufacturing. However, few breakthroughs have been achieved on the fabrication of interconnect membranes. As mentioned in the literature [13], there are few reports about dense doped lanthanum chromite ceramic interconnect membrane on porous anode support by the potentially cost-effective co-firing process. Wang et al. fabricated a dense $La_{0.7}Ca_{0.3}CrO_3$ interconnect thin membrane on $NiO/Sm_{0.2}Ce_{0.8}O_{2-\delta}/La_{0.7}Ca_{0.3}Cr_{0.97}O_{3-\delta}$ anode substrates by co-firing [13]. They added some $La_{0.7}Ca_{0.3}CrO_{3-\delta}$ to anode composition to succeed co-firing of interconnect and anode. This study reports our efforts to prepare a novel bilayered $CaCrO_4/La_{1-x}Sr_xCrO_{3-\delta}$ interconnector via co-sintering with green NiO–YSZ anode. After sintering the $CaCrO_4/La_{1-x}Sr_xCrO_{3-\delta}$, bilayer interconnect transforms to a dense single layer as $La_{1-x-y}Sr_xCa_yCrO_{3-\delta}$ ($y < 0.2$) which has been studied by some researchers for SOFC interconnect material due to its good electrical conductivity and stability during cooling and heating cycles [14]. In addition, all powders were synthesized by glycine–nitrate process (GNP). This process has been introduced as one of general classes of combustion methods for the preparation of ceramic powders; and when compared to similar compositions made using other processes, glycine–nitrate-produced powders had greater compositional uniformity, lower residual carbon levels and smaller particle sizes [15]. The sintering character, microstructure and electrical conductivity were also investigated.

2. Experimental procedures

$La_{1-x}Sr_xCrO_3$ specimens were prepared by glycine–nitrate process (GNP) [15]. The starting materials were glycine (as the fuel); La, Sr, Ca and Cr nitrates (as the

* Corresponding author. Tel.: +98 0311 3915744; fax: +98 0311 3912751.
E-mail address: a.heidarpour@gmail.com (A. Heidarpour).

0925-8388/$ – see front matter © 2011 Elsevier B.V. All rights reserved.
doi:10.1016/j.jallcom.2011.09.055

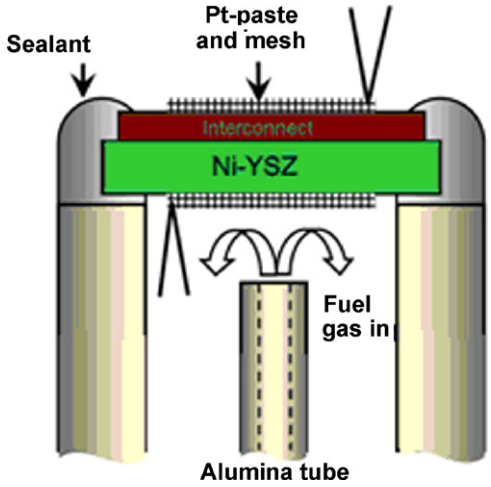

Fig. 1. Schematic illustration of the electrical measurement set-up for the anode-supported SOFC.

oxidant) which were of analytical purity. Solutions of La, Sr, Ca and Cr, nitrates were prepared and calculated stoichiometric amounts of glycine ($C_2H_5NO_2$) were added to synthesize $La_{1-x}Sr_xCrO_3$ (x = 0.1, 0.2 which were named as LSC10 and LSC20 respectively). The solutions were then boiled to evaporate excess water. The resulting viscous liquids were ignited in a hood in 1 l stainless-steel beaker on a hot plate and underwent self-sustaining combustion, producing an ash composed of the oxide product. It was found that the ratio of glycine to metal had a significant effect on the properties of prepared powders. Stoichiometric ratio has been reported as optimum ratio [16], and this ratio was chosen in this work, too. By this method, $La_{0.7}Ca_{0.3}CrO_3$ (LCC) and $CaCrO_4$ (CC) were also synthesized. For homogenization, the synthesized powder was milled in ethyl alcohol for 6 h with zirconia balls (10 and 5 mm diameter) at 100 rpm, and the powders were calcined at 500 °C for 30 min to remove any organic residuals. Phase determination in the samples was carried out by means of an XRD-Rigaku diffractometer using Cu K_α radiation (λ = 1.5406 Å). The specific surface area of the samples was measured by liquid nitrogen adsorption–desorption isotherms at 77 K on a Micrometrics ASAP 2010 system after degassing at 120 °C. NiO powder (99.97%, Kojundo Chemical, Japan) and YSZ powder (TZ-8YS, 99.9%, Tosoh, Japan) were used as the starting materials to synthesize NiO–YSZ composite as anode. Ten weight percent of corn starch was added as a pore former for the anode substrates. NiO and YSZ at the weight ratios of 6:4 were milled for 18 h in ethanol, and dried subsequently. The composite powders were then die-pressed (25 mm diameter) and pre-sintered at 950 °C for 1 h. In order to process interconnect thin membrane, the doped lanthanum chromites were coated on top surface of a supporting NiO–YSZ pre-sintered pellet by screen printing. The screen printing paste was made by mixing the powder with alpha-terpineol, ethyl cellulose and ethylene glycol. All pastes were 3-roll milled (EXAKT 50, Exakt, Germany) for uniform powder distribution. The cell was co-fired at 1400 °C for 3–10 h to obtain a dense lanthanum chromite base interconnect layer. Microstructures of the sintered bodies and interconnect membranes were observed using a field emission scanning electron microscope JEOL-JSM-6330F equipped by EDS microanalyzer. The co-sintered anode and interconnect was then glass sealed to an alumina tube for electrical conductivity tests (Fig. 1). The electrical conductivity was tested at 800 °C with 97%H_2–3%H_2O gas (100 cm^3 min^{-1}) as a fuel and air (open air) as an oxidant gas. Pt paste (No.6082, Engelhard, USA) and Pt mesh (52 mesh, Alpha Aesar, USA) as a current-collector were attached to the sintered body. An impedance analyzer (Solartron Instruments 1260, UK) was used to evaluate the electrode resistance and ohmic resistance. The impedance spectra were obtained under open circuit conditions with amplitude of 0.5 V in the frequency range 0.1 Hz to 50 kHz. The reason for conducting impedance measurements with amplitude of 0.5 V was to ensure that if there was polarization on impedance spectra or not. The electrical measurement was performed after reduction of NiO in anode for 5 h in 97%H_2 + 3%H_2O gas at 800 °C by using a set-up shown in Fig. 1. Ohmic resistance and area specific resistance (ASR) were measured by impedance spectra. The obtained resistance was considered as interconnect resistance because anode had Ni in its composition and its resistance was negligible. Actually the resistance and ASR of interconnect membrane were measured in dual atmosphere. The amount of gas leakage through sintered film was measured at room temperature [17]. The amount of gas leakage across the sintered films was characterized by gas flow rate measurements. The room temperature method essentially compares the inlet flow with the outlet flow resulting in a measured gas flow rate of air that is lost through the sintered film. Mean gas permeance values were calculated from measurements on at least five samples for each fabrication method to reduce the potential errors associated with the porous substrate and fabrication of the screen-printed layers.

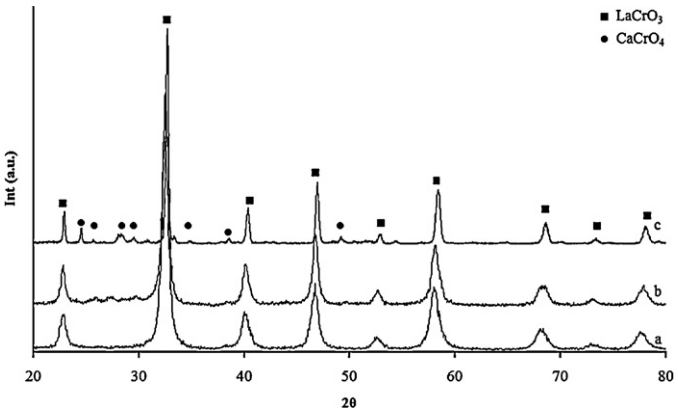

Fig. 2. XRD patterns of synthesized powder: (a) LSC10, (b) LSC20 and (c) LCC30.

3. Results and discussion

3.1. Synthesis and characterization of powders

Fig. 2 shows the XRD patterns of LSC10, LSC20 and LCC powders at room temperature. It reveals the perovskite structure, and in particular formation of single perovskite phases in the LSC10 and LSC20 powders while in the case of LCC, some $CaCrO_4$ is found. $CaCrO_4$ is exsoluted due to poor solid solubility in the perovskite at low temperatures (below ~1300 °C) because GNP synthesis is fast and the temperature reached is not sufficient to dissolve a second phase. So, this phase was considered as an intermediate phase. The crystal system of all doped lanthanum chromite samples was orthorhombic. The specific surface area of all samples was about 22 m^2/g. In addition, EDS was used to confirm the chemical composition of powders.

3.2. Doped lanthanum chromite membrane

The LSC10, LSC20 and LCC interconnect powders were made into slurry by being mixed with the binder and organic solvent before screen printing. All the samples were screen-printed on pre-sintered NiO–YSZ anode and co-fired. Unfortunately, and as expected, all the samples were porous. Fig. 3 shows the cross-sectional view of LCC interconnect film sintered at 1400 °C. The porosity estimated using SEM was about 30–40%. The densification of the screen-printed interconnect films was restricted at this

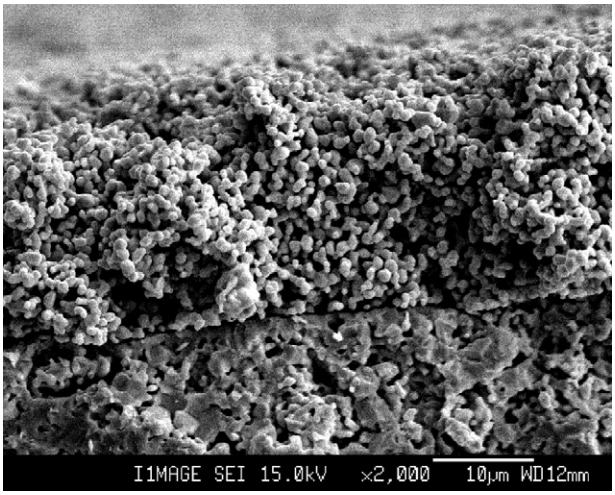

Fig. 3. Cross-section SEM micrograph of co-sintered LCC30 interconnect and anode at 1400 °C for 10 h.

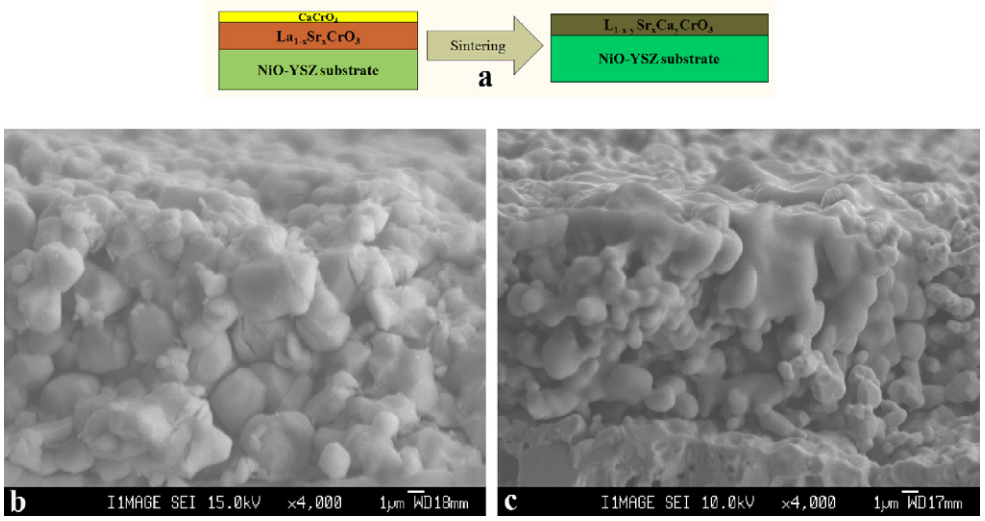

Fig. 4. (a) Schematic representation of bilayer interconnect and anode before and after sintering, (b) and (c) cross-section SEM micrographs of LSC20/CC with 30 μm and 50 μm CC top layer thickness, respectively.

temperature because of evaporation of chromium species and difficulty of diffusion [18,19]. In the case of LSC10 and LSC20, they were hardly sintered at 1500 °C as bulk samples, but LCC30 sample was easily sintered at 1400 °C as a bulk sample [19]; however, it did not densify as a thick layer on top of a porous substrate. Wang et al. [13] reported successful densification of LCC30 by adding some LCC30 (~30%) to anode, and claimed that it prohibited chromium evaporation and encouraged densification.

As a sintering mechanism of doped lanthanum chromite, it is suggested that liquid phase forming species like $CaCrO_4$ help sintering and densification. This species melt and dissolve in $LaCrO_3$ during sintering. If the amount is low, it disappears and no second phase can be detected [19]. In our attempt, we used a two-layer system (Fig. 4a), one being LSC10 and LSC20, and $CaCrO_4$ as the top layer. LSC10 and LSC20 were chosen because these compositions can dissolve more doping elements before saturation.

Two composite layers were chosen as LSC10/CC and LSC20/CC. The screen-printing process with mesh size screen thickness was used to change the thickness of the laminate prior to sintering. The thickness of base layer (LSC10 or LSC20) was constant at 30 μm while two thicknesses of 30 and 50 μm were used for the top layer ($CaCrO_4$, CC). Co-sintering was conducted at 1400 °C for 3, 5 and 10 h. Based on gas leakage test, the LSC10/CC bilayer after sintering at 1400 °C for 10 h, was porous. So, it was left out of investigation. For LSC20/CC composite layer sintered at 1400 °C for 5 and 10 h, the gas leakage was negligible and was investigated by SEM. Fig. 4 shows the SEM micrographs of co-sintered interconnector and anode. As shown, the interconnector layer with initial 30 μm CC top layer was about 10 μm and was quite dense despite the presence of a few closed pores. In the case of 50 μm CC top layer, some liquid sank down to the bottom and mixed with substrate which was undesirable.

XRD pattern tested on the final membrane surface is shown in Fig. 5. The interconnect layer shows pure rhombohedral perovskite structure, indicating no other phase. In this figure, patterns of LSC20, $CaCrO_4$ are shown for comparison. As can be seen, LSC20 has an orthorhombic crystal structure while after co-sintering, the final layer is rhombohedral. It is shown that the crystal system of specimens with larger Sr content in $La_{1-x}Sr_xCa_yCrO_3$ is rhombohedral [14]. In addition, it has been reported that the crystal structure of $LaCrO_3$ changes from orthorhombic distorted perovskite to rhombohedral at 250 °C [20]. The structural phase transition involves discrete volume variation and decrease in mechanical strength between room and SOFC operation temperature. Sakai and coworkers investigated the phase transition behavior of $La_{1-x}Ca_xCrO_3$ and concluded that phase transition temperature increased with an increase in Ca content [21–23]. Nakamura et al. reported the phase transition behavior of $La_{1-x}Sr_xCrO_3$ [24]. According to their work the temperature and variation of enthalpy at the structural phase transition decreases with Sr content. Therefore, it can be concluded that in $La_{1-x}Ca_xCrO_3$ ceramics with high density reported so far [23], Sr should be substituted to change the structural phase transition from room to SOFC operation temperature. So, we used the bilayer technique to fabricate dense $La_{1-x}Sr_xCa_yCrO_3$ ($x \sim 0.2$ and $y \sim 0.1$) layer with no structural phase transition. Although Wang et al. [13] fabricated a dense $La_{0.7}Ca_{0.3}CrO_3$ (LCC) interconnect thin membrane on anode substrate by co-firing, LCC has orthorhombic to rhombohedral phase transition in room temperature to SOFC operation temperature range. So, this composition is not good for application.

The ohmic resistance between anode and interconnector at 800 °C was measured as 0.0089 Ω cm^2, which is smaller than the resistances of SLT/LSM (0.265 Ω cm^2) [25] and LSTF (~0.03 Ω cm^2) [26] at the same temperature. The ohmic resistance significantly decreases at higher temperatures showing that ceramic interconnectors are more advantageous at high temperatures. In addition,

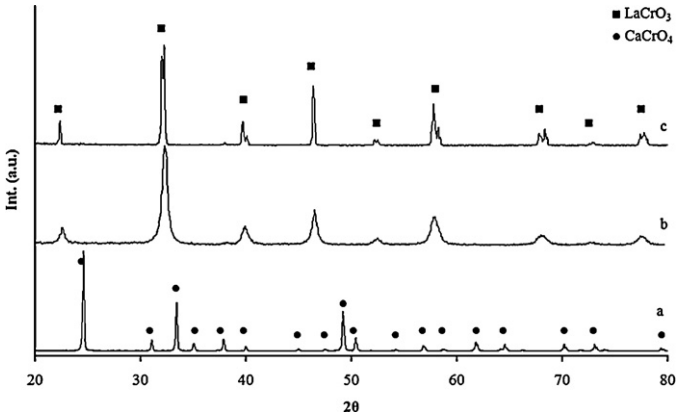

Fig. 5. XRD patterns of (a) $CaCrO_4$, (b) LSC20 and (c) final layer (LSC20/CC) after sintering at 1400 °C for 10 h.

electrical conductivity test was continued for 24 h and no change was observed in resistance.

4. Conclusions

The main results obtained from this research work can be concluded as follows:

1. A novel approach to co-sintering of doped lanthanum chromite interconnects on Ni–YSZ anode substrate for SOFC applications was developed. In this method, two layers of $La_{1-x}Sr_xCrO_{3-\delta}$ and $CaCrO_4$ (as top layer) were applied on NiO–YSZ substrate and then co-sintered.
2. SEM micrographs showed that LSC20/CC bilayer combined well together by the same thickness which sintered at 1400 °C for 10 h. In this situation, the gas leakage was negligible which proves that the layer was quite dense.
3. By using the bilayer technique, a dense $La_{1-x}Sr_xCa_yCrO_3$ ($x \sim 0.2$ and $y \sim 0.1$) layer was fabricated with no orthorhombic to rhombohedral phase transition.
4. Area specific resistance between anode and interconnector at 800 °C in dual atmosphere was about 0.009 $\Omega\,cm^2$ which is smaller than the resistances of other interconnect compositions at the same temperature. In addition, no change was observed in resistance up to 24 h.

References

[1] J.H. Kim, R.H. Song, K.S. Song, S.H. Hyun, D.R. Shin, H. Yokokawa, J. Power Sources 122 (2003) 138–143.
[2] K. Park, C. Lee, J. Bae, Y. Yoo, Int. J. Hydrogen Energy 34 (2009) 6861–6868.
[3] S.W. Baek, J. Jeong, J.H. Kim, C. Lee, J. Bae, Int. J. Hydrogen Energy 35 (21) (2010) 11878–11889.
[4] N. Droushiotis, U. Doraswami, K. Kanawka, G.H. Kelsall, K. Li, Electrochem. Commun. 11 (2009) 1799–1802.
[5] N.H. Menzler, F. Tietz, S. Uhlenbruck, H.P. Buchkremer, D. Stöver, J. Mater. Sci. 45 (12) (2010) 3109–3135.
[6] T. Yamaguchi, S. Shimizu, T. Suzuki, Y. Fujishiro, M. Awano, Electrochem. Commun. 10 (2008) 1381–1383.
[7] U.B. Pal, Solid State Ionics 52 (1992) 227–233.
[8] J.W. Fergus, Solid State Ionics 171 (2004) 1–15.
[9] S. Wang, B. Lin, Y. Chen, X. Liu, G. Meng, J. Alloys Compd. 479 (2009) 764–768.
[10] B. Lin, S. Wang, X. Liu, G. Meng, J. Alloys Compd. 490 (1-2) (2010) 214–222.
[11] C. Yamaqata, S.R.H. Mello-Castanho, Mater. Sci. Forum 660–661 (2010) 971–976.
[12] Y.P. Fu, H.C. Wang, S.H. Hu, K.W. Tay, Ceram. Int. 37 (7) (2011) 2127–2134.
[13] S. Wang, Y. Dong, B. Lin, J. Gao, X. Liu, G. Meng, Mater. Res. Bull. 44 (2009) 2127–2133.
[14] A. Mitsui, K. Homma, Y. Kumekawa, F. Nakamura, N. Ohba, Y. Hoshino, T. Hashimoto, J. Electrochem. Soc. 155 (5) (2008) A395–A403.
[15] L.A. Chick, L.R. Pederson, G.D. Maupin, J.L. Bates, L.E. Thomas, G.J. Exarhos, Mater. Lett. 10 (1990) 6–12.
[16] S.R. Nair, R.D. Purohit, A.K. Tyagi, P.K. Sinha, B.P. Sharma, Mater. Res. Bull. 43 (2008) 1573–1582.
[17] G.J. Wright, J.A. Yeomans, J. Eur. Ceram. Soc. 28 (2008) 779–785.
[18] S. Simner, J. Hardy, J. Stevenson, T. Armstrong, J. Mater. Sci. 34 (1999) 5721–5732.
[19] L.A. Chick, J. Liu, J.W. Stevenson, T.R. Armstrong, D.E. McCready, G.D. Maupin, G.W. Coffey, C.A. Coyle, J. Am. Ceram. Soc. 80 (8) (1997) 2109–2120.
[20] T. Hashimoto, N. Tsuzuki, A. Kishi, K. Takagi, K. Tsuda, M. Tanaka, K. Oikawa, T. Kamiyama, K. Yoshida, H. Tagawa, M. Dokiya, Solid State Ionics 132 (2000) 181–188.
[21] N. Sakai, T. Kawada, H. Yokokawa, M. Dokiya, T. Iwata, Solid State Ionics 394 (1990) 40–41.
[22] N. Sakai, S. Stølen, J. Chem. Thermodyn. 27 (1995) 493–506.
[23] N. Sakai, H. Fjellvag, B.C. Hauback, J. Solid State Chem. 121 (1996) 202–213.
[24] F. Nakamura, Y. Matsunaga, N. Ohba, K. Arai, H. Matsubara, H. Takahashi, T. Hashimoto, Thermochim. Acta 435 (2005) 222–229.
[25] Y. Xu, S. Wang, R. Liu, T. Wen, Z. Wen, J. Power Sources 196 (2011) 1338–1341.
[26] Y. Takahashi, A. Kawahara, T. Suzuki, M. Hirano, W. Shin, Solid State Ionics 181 (2010) 300–305.